ELSEVIER

Journal of Fluids and Structures 25 (2009) 889–896

JOURNAL OF FLUIDS AND STRUCTURES

www.elsevier.com/locate/jfs

Brief Communication

Influence of inlet shear on the 3-D flow past a square cylinder at moderate Reynolds number

A. Lankadasu, S. Vengadesan*

Department of Applied Mechanics, IIT Madras, Chennai 600036, India

Received 3 October 2008; accepted 4 April 2009
Available online 19 May 2009

Abstract

Unsteady three-dimensional (3-D) numerical simulations of linear shear flow past a square cylinder at moderate Reynolds number (Re = 200) are performed. The shear parameter (K) considered in this study is varied as 0.0, 0.1, and 0.2. For the uniform flow ($K = 0.0$) case, the chosen Re falls in the transition Reynolds number range. The low frequency force pulsations of square cylinder transition phenomena are observed to decrease with increasing shear parameter. The evolution of streamwise vortical structures indicates a mode A spanwise instability in the uniform flow. Unlike in uniform flow, mixed mode A and mode B spanwise instability is observed in the case of a shear flow. The autocorrelation function of the lift and the drag coefficients is improved for any particular separation distance with increasing K.
© 2009 Elsevier Ltd. All rights reserved.

Keywords: Square cylinder; Cross-flow; Inlet shear

1. Introduction

Uniform flow past a bluff body has been a subject of research for many decades. Though many experimental and numerical simulations of the transition of a two-dimensional (2-D) wake to a three-dimensional (3-D) wake have been reported, the origin, structure, and the role these transitions play on the flow parameters has not yet been made clear. With the increase in computational capabilities and advanced experimental and analytical techniques, researchers have recently gained insights into vortex dislocations, and mode A and mode B instabilities (Williamson, 1996). Mode A and mode B instabilities are quite distinct in the spanwise length scale. Mode A instability has a spanwise wavelength of about three to four cylinder diameters, whereas mode B is characterized by a shorter spanwise wavelength of about one cylinder diameter. The existence of these two transition modes has been confirmed by experimental, numerical, and analytical approaches. From the literature, it is observed that the Re corresponds to the inception of mode A and mode B instabilities; for the case of uniform flow, it is reported differently in different studies. However, the numbers fall in the range of $190 < Re < 240$ and $Re > 240$, respectively.

In practice, many structures, such as offshore structures and pipelines near the seabed, are immersed in a boundary layer. When a small cylinder is placed in the shear layer of a large main cylinder to alter the vortex-shedding phenomena behind the main cylinder, the small cylinder is inevitably subjected to the effect of shear induced from the larger

*Corresponding author. Tel.: +91 44 22574063; fax: +91 44 22574052.
E-mail address: vengades@iitm.ac.in (S. Vengadesan).

0889-9746/$ - see front matter © 2009 Elsevier Ltd. All rights reserved.
doi:10.1016/j.jfluidstructs.2009.04.003

cylinder. These are typical cases with non-uniform approach flow. The simplest case of a non-uniform approach flow is the uniform shear flow, which has a linear distribution of the longitudinal velocity component along the transverse direction. It has been shown by past investigations on circular cylinders (e.g., Kang (2006), Cao et al. (2007) and references cited therein), that flow approaching with linear shear alters the vortex dynamics in the wake when compared to that of the uniform flow case. However, much less work has been reported on square cylindrical bodies (e.g., Cheng et al. (2007) and references cited therein). It should be noted that all of the above numerical studies are restricted to 2-D simulations. The observations reported in the above studies have motivated us to investigate the effect of shear on the development of three-dimensionality in the wake of a square cylinder.

The main objective of the present study is to investigate the effect of shearing approach flow past a square cylinder at the transition Reynolds number of $\mathrm{Re} = 200$. The transition process is inherently a 3-D process, and 2-D simulation cannot predict signatures of transition phenomenon. To this end, unsteady 3-D numerical simulations are performed with an inlet shear parameter of $K = 0.0$, 0.1, and 0.2 and the associated wake transition process is reported in detail.

2. Problem statement and numerical method

The problem under consideration in the present study is 3-D, unsteady, viscous and incompressible flow with constant fluid properties around an isolated square cylinder. The governing equations for the present flow configuration are the respective Navier-Stokes equations. All geometrical lengths are normalized with the size of cylinder side d, velocities with the speed of the undisturbed stream at the center of the cylinder U, physical times with d/U, and pressure with ρU^2, with ρ as the fluid density. The coefficient of drag and Strouhal number (St) are defined as $\bar{C}_D = 2\bar{F}_D/\rho U^2 A$ and $\mathrm{St} = fd/U$, respectively, where $\bar{F}_D$ is the mean drag force, f is the shedding frequency, and A is the facing area equal to the $d \times Z$. Fig. 1 shows the schematic diagram of the flow configuration. The first grid point from the body is maintained at $0.008d$. In the present study, the residual of the continuity equation for mass conservation on each cell was set at a maximum value of 0.0005.

At the inlet, a linear velocity profile ($u = 1 + Ky$, $v = w = 0$) is assumed, where K is a nondimensional shear parameter ($K = Gd/U$), and G is the gradient of streamwise velocity component in the lateral direction ($\mathrm{d}u/\mathrm{d}y$). At the outlet boundary, the convective boundary condition ($\partial u_i/\partial t + U_c(\partial u_i/\partial x_j) = 0$) is used for all velocity components, where U_c is the convective speed and, in the present work, is space-averaged streamwise exit velocity. No-slip conditions are prescribed on the body surface. At the top and bottom, we use $\partial u/\partial y = K$, $\partial w/\partial y = 0$, $v = 0$ (Kang, 2006; Lankadasu and Vengadesan, 2008a, b). It should be noted that if the K value is zero, this condition results in the symmetry condition. In the spanwise direction, a periodic boundary condition is employed.

To avoid a negative velocity at the inlet we confine the study to either high blockage ratio or low shear parameters (Kang, 2006). In the present study, the lateral width, w, of the domain is 10 times the cylinder width, d, for all shear parameters. For this lateral width, the solid blockage ratio calculated using $B = d/w$ is 10%. Based on the present blockage ratio, the maximum shear parameter has been restricted to $K = 0.2$.

Studies on the influence of the first grid point from the cylinder, length of inlet, and the outlet domain have been reported in previous work (Lankadasu and Vengadesan, 2008a, b). The same grid and computational domain, used in the authors' earlier 2-D work ($-8d < x < 20d$ and $-5d < y < 5d$) are now extended in the spanwise direction to $8d$ in the present 3-D simulation with 41 uniformly placed grid points. The present spanwise width can accommodate two pairs

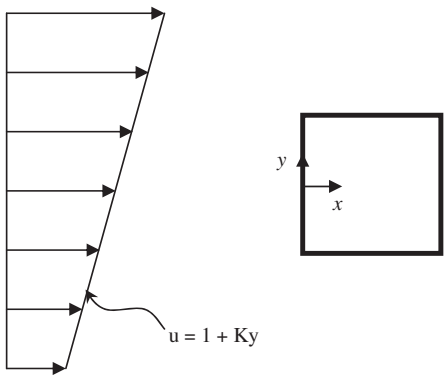

Fig. 1. Schematic of the flow configuration and coordinate system.

Table 1
Comparison of bulk parameters with previously reported values for $Re = 200$, $K = 0.0$, where Z is the spanwise width.

Author	K	Z	$\bar{C}_D$	$C_{L,\mathrm{rms}}$	$C_{D,\mathrm{rms}}$	St
Sohankar et al. (1999)	0.0	6	1.39	0.21	0.032	0.157
Sohankar et al. (1999)	0.0	10	1.41	0.22	0.023	0.160
Robichaux et al. (1999)	0.0	–	1.64	–	–	0.157
Present ($226 \times 195 \times 41$)	0.0	8	1.563	0.35	0.034	0.159
Present ($226 \times 195 \times 41$)	0.1	8	1.553	0.167	0.0054	0.152
Present ($226 \times 195 \times 41$)	0.2	8	1.569	0.182	0.0128	0.152
Present ($226 \times 195 \times 65$)	0.2	8	1.574	0.2078	0.0184	0.152

of secondary vortices for mode A spanwise instability in uniform flow and is also higher than that used by Sohankar et al. (1999). This group further increased the spanwise length from $6d$ to $10d$ and found a decrease in the sectional r.m.s. drag, but insignificant effects on Strouhal number, mean drag coefficient, and r.m.s. lift. Further, in order to assess the influence of spanwise resolution on the results, a flow configuration of $K = 0.2$ has been studied and results are presented in Table 1. The number of nodes in the spanwise direction is now increased from 41 to 65 for the same $8d$ length. The bulk parameters show a very small decreasing trend, but the corresponding increase in computational time is twice that of the former grid. Hence, the remaining calculations are carried out with $8d$ and 41 nodes in the spanwise direction. The final grid and domain size are $226 \times 195 \times 41$ and $30d \times 10d \times 8d$, respectively.

Global parameters such as mean drag coefficient, root mean square value of the lift and drag coefficients, and Strouhal number calculated using the present grid and the computational domain with uniform flow over a square cylinder and their typical results are compared with the available literature for $Re = 200$ in Table 1. Further, it is not known that boundary conditions, domain size, grid resolution, and numerical schemes have an influence on the results. Considering all these factors, the present results seem to be in general agreement with those of the literature.

3. Results and discussion

In the present study, numerical simulations were performed for incoming linear shear flow past a square cylinder. The shear parameter, K, is varied as 0.0, 0.1, and 0.2. The solution begins with an initial condition of the fluid at rest throughout the computational domain, except at the inlet boundary, where the prescribed linear velocity profile is forced. The solution is allowed to march forward in time until it is stabilized, which is observed from the time variation of spanwise averaged lift and drag coefficients. After this, the results in terms of instantaneous lift and drag coefficient and their autocorrelations, instantaneous isosurfaces, and time-averaged pressure contours are presented and discussed in this section.

3.1. Instantaneous lift and drag coefficient and their autocorrelations

The spanwise averaged lift and drag coefficients are shown in Fig. 2. For the Re considered in this study, bluff body flow such as that around like circular and square cylinders and normal flat plates shows low-frequency unsteadiness over and above the von Karman shedding. For the case of a square cylinder, this unsteadiness begins at $Re = 175$ and fades with increasing Re. The Re considered in the present study falls in this range. The unusual intermittent low-frequency modulation can be related to the vortex dislocation, triggered by the boundary conditions (Williamson, 1996). Consequently, mean lift and drag coefficients become low at that time. Low-frequency unsteadiness is observed in both lift and drag coefficients for $K = 0.0$. The decrease of the drag coefficient during the period of vortex dislocation is due to a longer recirculation length compared to that of the regular shedding mode. The r.m.s. value of the drag coefficient is very low compared to that of the lift coefficient. The r.m.s. fluctuations momentarily decrease during vortex dislocation. With further increase in the Reynolds number, intermittent low-frequency modulation in the flow decreases, and the pulsation phenomenon fades out. Averaged values of the lift and drag coefficients are compared with those from the available literature in Table 1 and are found in good agreement.

The spanwise averaged instantaneous lift and drag coefficient for shear parameter $K = 0.2$ are depicted in Fig. 2(a). The r.m.s. value of both lift and drag coefficients ($C_{L,\mathrm{rms}}$, $C_{D,\mathrm{rms}}$) increases with increasing K. This trend is qualitatively consistent with the 2-D simulations of Saha et al. (1999) at a slightly higher value of $Re = 250$, but deviates distinctly

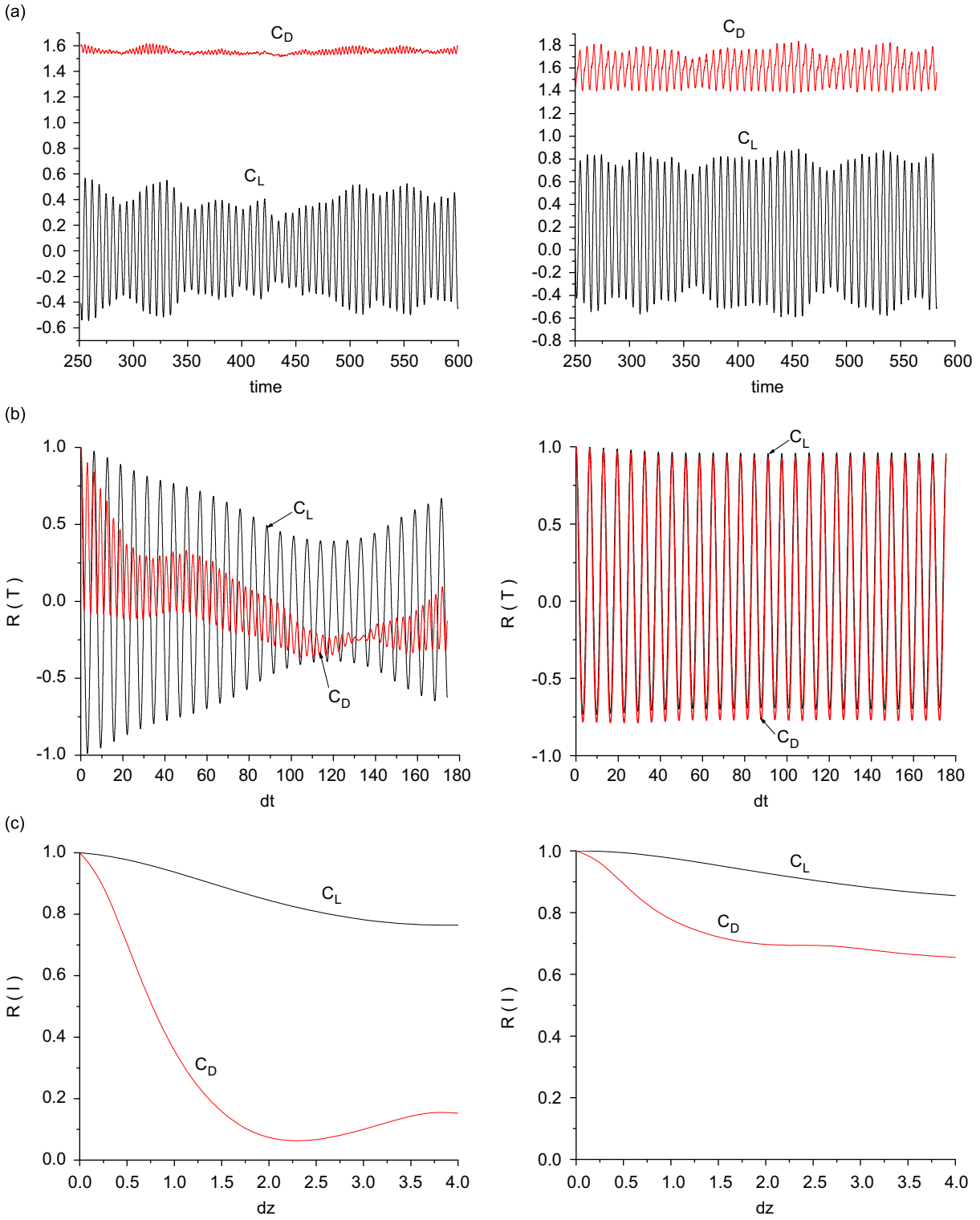

Fig. 2. Autocorrelation of lift and drag coefficients: (a) lift and drag coefficients, (b) autocorrelation in the time series, and (c) autocorrelation along the spanwise direction. Left side for $K = 0.0$ and right side for $K = 0.2$.

from the low blockage ratio (4%) 2-D results of Cheng et al. (2007) at Re = 200. The trend in $C_{L,\mathrm{rms}}$, $C_{D,\mathrm{rms}}$ could be due to velocity differences between the top and bottom sides of the cylinder, which increase with increasing shear. This leads to the corresponding pressure variations on both sides. Because of this, the amplitude of the lift coefficient increases on the positive side, whereas it remains the same on the negative side of the mean, as in the case with $K = 0.0$. This trend could be attributed to the increased transverse velocities with increasing K. This results in a positive mean lift coefficient. For the case of shear flow, the direction of the mean lift coefficient has been reported differently in flow past a circular cylinder. In the case of a solid sphere, the mean lift force acts from the lower velocity side to the higher velocity side for low to moderate Reynolds number flows, whereas it acts in the opposite sense for moderate to high Re. For a spherical bubble, lift acts from the lower to higher velocity direction irrespective of Re. The circular cylinder shows this discrepancy in other reported studies. Kang (2006) studied the circular cylinder with a shearing approach flow at Re = 100 with different blockage ratios and found that the mean lift force acts from the high-velocity side to the low-velocity side. He finally concluded that the effect of the blockage ratio on the drag and lift is on the order of that due to the shear parameter. The possible discrepancy in the direction of the mean lift could be due to the difference in blockage ratio in the previous studies. For the square cylinder Cheng et al. (2007) recently reported a negative lift coefficient for the Reynolds number range from 50 to 200 and shear parameter range from 0.0 to 0.4, with the remaining all reporting a positive lift coefficient. Moreover, all of the above numerical results are 2-D. Our present 3-D simulations at Re = 200 show a positive lift coefficient when $K > 0.0$. To test the influence of three-dimensionality on the mean lift coefficient, 2-D simulations are also performed for the same Re, shear parameters, and blockage ratio. In all cases a positive lift coefficient was observed. The major difference among square cylinder studies is in the blockage ratio used. Except for Cheng et al. (2007), all others used a high blockage ratio (i.e., velocity at the inlet is positive for all shear parameters considered in their respective studies). As pointed out in Kang (2006), for high blockage, the influence due to blockage ratio prevails over that due to the shear parameter. From the above studies, one can observe that the discrepancy in the mean lift coefficient could be due to any one or a combination of the following factors: blockage ratio, Reynolds number, fixed separation point (in case of a square cylinder), and three-dimensional effects. At this moment, it is difficult to pinpoint the exact reason for the discrepancy among these studies. The influence of shear parameter on bulk parameters is presented quantitatively in Table 1.

In the study of bluff body flows, correlation time and length of lift and drag coefficients in the time and spanwise separation distances is very important. However, related studies in open literature are few. In the present work, the autocorrelation function of lift and drag coefficients is evaluated. Fig. 2(b) (left side) shows the autocorrelation of the lift and drag coefficients in the time series. Lift and drag signals are collected over a span of more than four low frequency cycles. The first peak in the lift correlation function is observed at a separation time of six and the corresponding frequency matches well with the shedding frequency of the Karman vortices. For the drag coefficient, the corresponding peak appears at a time of three, half of that in the lift correlation. This supports the fact that the shedding frequency of the drag is twice that of the lift in the case of uniform flow. Note that the drag correlation is done only for the fluctuating part after subtracting the mean from the instantaneous part. The second low-frequency peak for both lift and drag coefficient autocorrelation functions occurs at a separation time of about 50, which corresponds to the frequency of 0.02. The autocorrelation function of lift and drag coefficients for the $K = 0.2$ case is shown in Fig. 2(a) (right side). Significant differences in the autocorrelation function can be observed between the shear and no shear cases. The first peak of the autocorrelation function of both lift and drag coefficients for the $K = 0.2$ case is observed at the same separation time of $T = 6.57$, which is marginally higher than that in the no shear case. Further, the low-frequency wavelength in both lift and drag is diminished.

The autocorrelation functions of the lift and drag coefficients with spanwise separation distance are depicted in Fig. 2(b). Please note that the autocorrelation function is averaged over the spanwise distance, because of that, the maximum separation distance is restricted to the $4d$, although the actual spanwise length is $8d$. In the no shear case [Fig. 2(c) (left side)], the lift coefficient is correlated well for the considered spanwise separation distance, whereas drag correlation continuously decreases up to a separation distance of 2.2, then increases and attains a peak at around 3.7. This distance corresponds to the wavelength of mode A type of spanwise instabilities for the considered Re = 200. Sohankar et al. (1999) placed the spanwise wavelength at 3.3. In contrast, from the Floquet analysis, Robichaux et al. (1999) reported a spanwise wavelength of 5.22 for a Reynolds number of 162 ± 12. Luo et al. (2007) reported a value of 5.2 from a flow visualization study for Re = 162. The spanwise autocorrelation function for $K = 0.2$ is shown in Fig. 2(c) (right side). The lift coefficient is highly correlated as in the $K = 0.0$ case. The correlation function of the drag coefficient improves in the case of $K = 0.2$. There is no clear secondary peak in the correlation coefficient, but there is a bulge at around $l = 2.7$. This suggests that there is no distinct streamwise and lateral vorticity arranged in the spanwise direction as in the $K = 0.0$ case. This could be due to different strengths of vorticity present at the top and the bottom shear layers. The approximate local Reynolds number at the top and at the bottom leading edges (based on the cylinder width, d) are 220 and 180, respectively. The bottom local Reynolds number is located around the inception of mode

A type of instability, whereas the top Reynolds number is within the range of mode A instability. The combined effect could be manifested in the spanwise correlation function.

3.2. Vortical structures

Vortical structures play a major role in the wake transition scenario and proper identification and extraction of vortical structures are important in understanding their origin and dynamics. In this paper, we followed the $-\lambda_2$ method (Jeong and Hussain, 1995). This method separates the dynamically significant core region from the outer region and is also Galilean invariant. Fig. 3 depicts the isosurface of $\lambda_2 = 0$, for $K = 0.0$ and $K = 0.2$. Fig. 3(a) shows the case for $K = 0.0$ and Fig. 3(b) and (c) for $K = 0.2$. For uniform flow, only the top view is shown as it is symmetric. For shear flow $K = 0.2$, the top and the bottom views are shown separately. The flow takes place from left to right. Both cases, with and without shear, have three-dimensional structures at this Reynolds number, which connect the core region of two successive primary vortical structures. These are termed streamwise streaks and have contributions from both streamwise and lateral components of vorticity and two adjacent streaks rotating in opposite direction. Due to the limitation of the identification method, it is not possible to show the direction of rotation. However, the observation is consistent with previously reported studies on a square cylinder with uniform flow (Sohankar et al., 1999). The secondary vortical structures have a high wavelength of approximately $3.2d$. This wavelength is slightly less than the wavelength calculated from the autocorrelation of the drag coefficient, which is usually referred as a mode A type of instability. Note that these 3-D isosurfaces are plotted at a particular instant of time and their spacing is not uniform along the spanwise length. However, the wavelength calculated from autocorrelation of the drag coefficient is time and space averaged and hence, there exists a small difference between these two values.

Due to the difference in local Reynolds number between the top and the bottom sides, completely different patterns are observed on the top and the bottom sides of the cylinder. On the top side, secondary vortical structures have a low wavelength of approximately $1.2d$, which indicates a mode B type of instability. On the bottom side, higher wavelength secondary structures are observed, which come under the category of mode A type of instability. After mixing of these two shear layers, low wavelength streaks lose their identity and the flow is dominated by high wavelength streaks. For both shear and no shear cases, it is observed that primary vortices shed in parallel (Fig. 4).

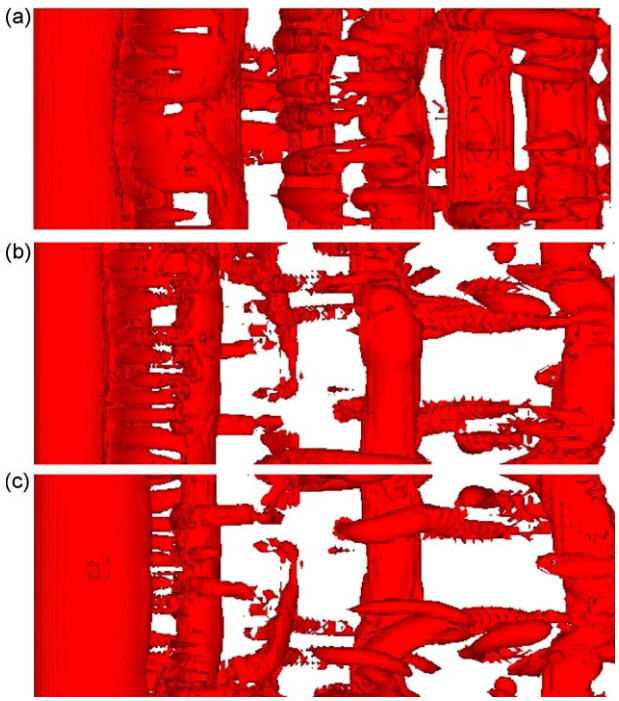

Fig. 3. Instantaneous iso-surface of $\lambda_2 = 0$: (a) $K = 0.0$, (b) top view, $K = 0.2$, and (c) bottom view, $K = 0.2$.

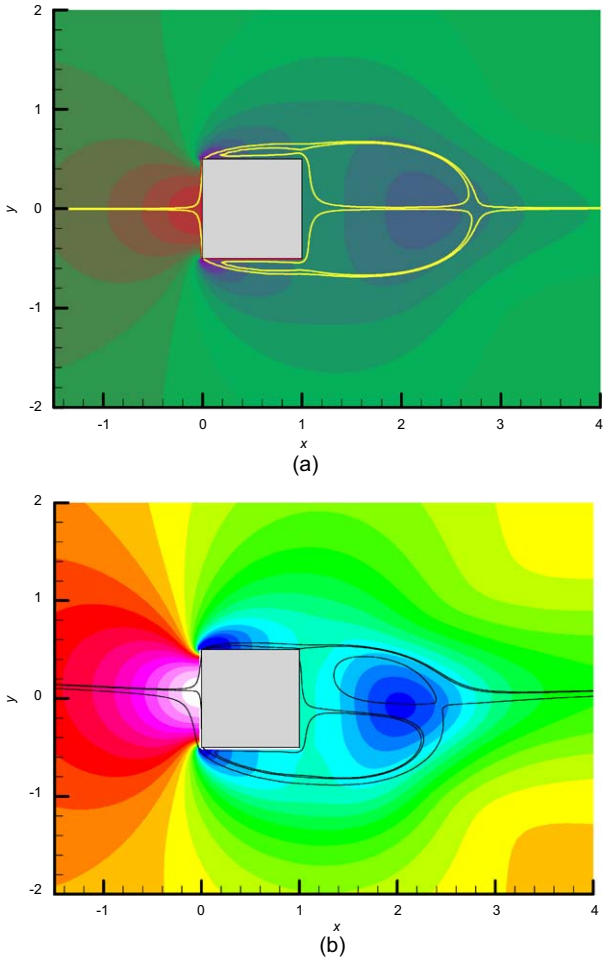

Fig. 4. Time and spanwise averaged pressure contours: (a) $K = 0.0$ and (b) $K = 0.2$.

3.3. Mean pressure

Time averaged pressure contours are depicted in Fig. 4. For qualitative information about the wake bubble, selected contours of stream function are superimposed on the pressure contours. When $K = 0.0$, it can be seen that the flow is separated from the leading edge and does not touch on the trailing edge. This is consistent with the work of Sohankar et al. (1999) who reported that, for $\mathrm{Re} > 175$ and in the fully saturated state, separation occurs from the leading corners. The mean recirculation length is about $2.74d$ which is in good agreement with the literature. The half-width of the bubble, defined as the maxima of the mean recirculation bubble from the centreline ($y = 0.0$) in the lateral direction, is approximately $0.68d$. The lowest pressure in the wake occurs at $2.22d$ from the origin. When $K = 0.2$, the wake bubble is not symmetric about the centerline, and the stagnation point on the front face shifts towards the top leading edge. The top shear layer separates from the leading edge and reattaches to the cylinder surface immediately. On the bottom side, the shear layer separates at the leading edge, and due to shear, it tilts towards the lower-velocity side. Because of this, the separated shear layer from the bottom side does not touch the trailing edge. The recirculation length is approximately $2.47d$ from the origin, which is less compared to that of the $K = 0.0$ case. The half-width of the bubble on the high velocity side is $0.55d$, and on the lower velocity side it is $0.88d$ from the centreline. The lowest pressure in the wake occurs approximately at $2.04d$. Furthermore, a recirculation bubble is formed on the bottom surface of the cylinder due to a higher pressure increase on the bottom surface as compared to that on the top side. Therefore, the net difference between the top and the bottom force coefficients results in the positive lift coefficient.

4. Conclusions

In the present study, time-dependent calculations for a three-dimensional flow around a square cylinder with linear shear at the inlet have been carried out. The purpose of the present study is to understand the influence of inlet shear on the 3-D flow past a square cylinder at moderate Reynolds number. The Reynolds number considered was $Re = 200$, and the inlet shear parameters considered are $K = 0.0$, 0.1, and 0.2. The spanwise correlation function of the lift coefficient is insensitive to the shear parameter. In contrast, the correlation function of the drag coefficient increases with increasing shear parameter. Furthermore, the spanwise wavelength decreases with increasing shear parameter. The 3-D isosurface of $\lambda_2 = 0$ reveals mode A and mode B types of instability on the lower and higher velocity side, respectively, for $K = 0.2$. In the case of uniform flow, only the mode A type of instability is observed. Thus, it is concluded that shear has an influence on the transition and thus on the bulk parameters. This is the first such reported 3-D study to consider the effect of inlet shear on the transition scenario.

References

Cao, S., Ozono, S., Hirano, K., Tamura, Y., 2007. Vortex shedding and aerodynamic forces on a circular cylinder in linear shear flow at subcritical Reynolds number. Journal of Fluids and Structures 23, 703–714.

Cheng, M., Whyte, D.S., Lou, J., 2007. Numerical simulation of flow around a square cylinder in uniform-shear flow. Journal of Fluids and Structures 23, 207–226.

Jeong, J., Hussain, F., 1995. On the identification of a vortex. Journal of Fluid Mechanics 285, 69–94.

Kang, S., 2006. Uniform-shear flow over a circular cylinder at low Reynolds numbers. Journal of Fluids and Structures 22, 541–555.

Lankadasu, A., Vengadesan, S., 2008a. Interference effect of two equal size square cylinders in tandem arrangement: with planar shear flow. International Journal for Numerical Methods in Fluids 57, 1005–1021.

Lankadasu, A., Vengadesan, S., 2008b. Onset of vortex shedding in planar shear flow past a square cylinder. International Journal of Heat and Fluid Flow 29, 1054–1059.

Luo, S.C., Tong, X.H., Khoo, B.C., 2007. Transition phenomena in the wake of a square cylinder. Journal of Fluids and Structures 23, 227–248.

Robichaux, J., Balachandar, S., Vanka, S.P., 1999. Three-dimensional Floquet instability of the wake of square cylinder. Physics of Fluids 11, 560–578.

Saha, A.K., Biswas, G., Muralidhar, K., 1999. Influence of inlet shear on structure of wake behind a square cylinder. Journal of Engineering Mechanics 125, 359–363.

Sohankar, A., Norberg, C., Davidson, L., 1999. Simulation of three-dimensional flow around a square cylinder at moderate Reynolds number. Physics of Fluids 11, 288–306.

Williamson, C.H.K., 1996. Three-dimensional wake transition. Journal of Fluid Mechanics 328, 345–407.